CHAPTER 4

Coal mine effluent treatment by semi-continuous cultivation of candidate microalgae in reactor scale*

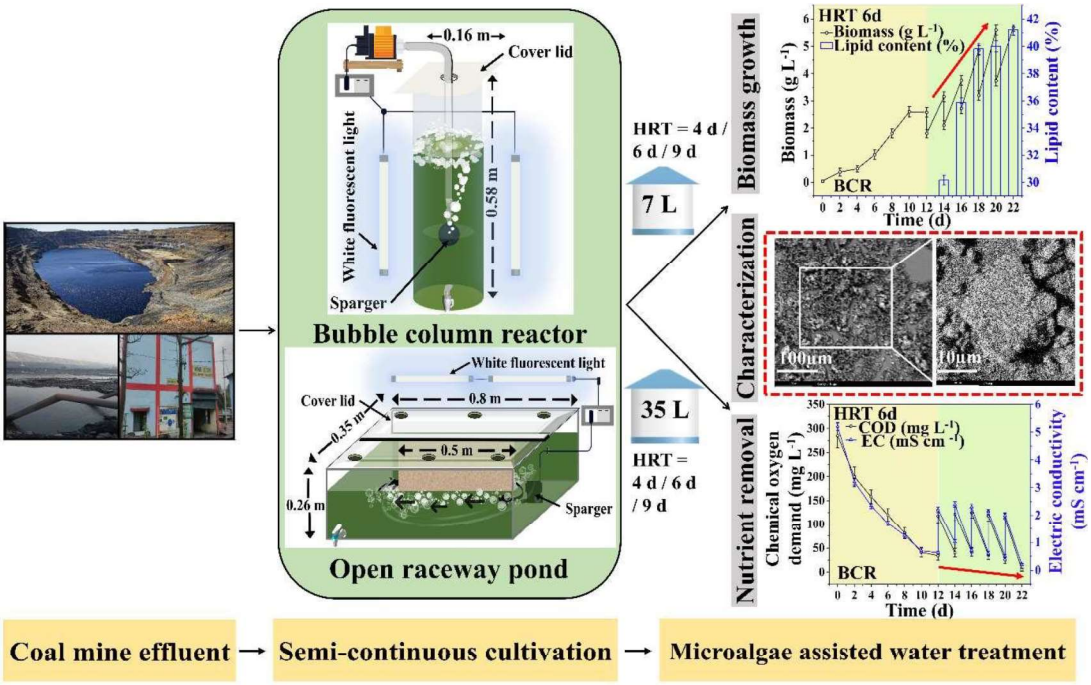

*This work is published in **Shweta Rawat, Agendra Gangwar and Sanjay Kumar (2024c)** Semi-continuous cultivation of microalgae to treat coal mine effluent in pilot scale: Nutrient removal, biodesalination and fatty acid composition analysis. Journal of water process engineering. 67, 106271.

Abstract

Coal mine water adversely affects the ecosystem; thus, treatment is required before discharging into the environment. Considering potentiality of microalgae for high salt tolerance, salt removal, and metallic pollutant removal from an aqueous system, present chapter focuses on the semi-continuous cultivation of candidate microalgae *C. pyrenoidosa* (NCIM 2738) in bubble column reactor (BCR) and open raceway pond (ORP) for nutrient supplemented coal mine effluent (NSCME) treatment. Between different hydraulic retention times (HRTs), HRT 6 d provides maximum average biomass productivity of 950 mg L^{-1} d^{-1} in BCR and 728.4 mg L^{-1} d^{-1} in ORP. HRT 9 d facilitates a maximum lipid content of 1.8 g L^{-1} in BCR and 1.4 g L^{-1} in ORP. Further, HRT 9 d had the maximum COD removal efficiency (96.5 % in BCR and 94.2 % in ORP) and maximum salinity removal efficiency (93 % in BCR and 92 % in ORP). Fatty acid methyl esters (FAME) characterization highlighted potential biodiesel applicability with cetane number (CN) of 53.94. Energy dispersive X-ray spectroscopy (EDS) revealed an excess amount of salt and metal ions deposition on the surface of harvested microalgae samples. Present chapter provides an outdoor large-scale *C. pyrenoidosa* cultivation strategy that can be integrated with coal mine closure plans to meet sustainable development goals (SDGs) 6, 7 and 13.

4.1. Background

This chapter focuses on the semi-continuous cultivation of candidate microalgae *C. pyrenoidosa* (NCIM 2738) in bubble column reactor (BCR) and open raceway pond (ORP) targeting NSCME treatment. Concerning recent developments in environmental, social and governance aspects in coal industries, exploitation of microalgal platforms for mine water treatment and desalination may be considered energy efficient, low cost and environmentally friendly practices for a longer time (Patel et al., 2021). Both microalgae cultivation systems, i.e., open or closed systems, play crucial roles in microalgal biomass production and water treatment performance (Arutselvan et al., 2022). Comparing both systems (closed and open), closed systems are relatively efficient due to upgraded process control, greater biomass productivity and reduced contamination risk (Arutselvan et al., 2022). In between different cultivation modes, a semi-continuous cultivation system is the most appropriate choice for large/pilot scale microalgae cultivation, which outperforms batch/ continuous systems (Tan et al., 2021). Although batch cultures are simple, flexible and easy to operate, it requires maintaining strain inoculum and cleaning reactors between runs, which increases consumables and results in lower productivity. In comparison to conventional batch cultivation, sequential batch and semi-continuous cultivation offers high nutrient removal efficiencies, consistent biomass productivity and lower cost (Rawat et al., 2024c). Further, such cultivation mode results biomass production and valuable biomolecule accumulation simultaneously in the same reactor with negligible downtime than batch mode.

In recent years, semi-continuous cultivation mode was successfully implemented to treat different types of waste water using the microalgal platform. In this direction, long-term semi-continuous cultivation of microalgae consortium (*Geitlerinema* sp. and *Coellastrella* sp.) is reported to treat low loaded domestic wastewater with 90% NH_4^+ removal and 57% DCW

accumulation (Salinas et al., 2021). In another study, fresh piggery wastewater was treated in open raceways using a microalgae consortium with maximum biomass production of 4.98 × 10^6 cell mL^{-1} and lipid productivity of 189.78 mg L^{-1} (Linares et al., 2020). The microalgae assisted wastewater treatment facilitates sustainable, low-cost processing technology for efficient salt ions/trace elements removal and microalgal biomass production for biofuels and other high value biochemicals (Mirzaei et al., 2024). The *D.* salina was investigated to remove heavy metals Cd, Pb and Cr with up to 95% removal efficiencies from contaminated water resources (Elleuch et al., 2021). Further, microalgal consortia (*Scenedesmus bijugatus*, *Oscillatoria*, *Nannochloropsis* sp., *Chlorella* sp., *C. reinhardtii* and *Oscillatoria*) is investigated to treat sewage wastewater with heavy metal removal efficiency of 85.06% Cu, 98.2% Pb, 99.6% Cd, 75.2% Cr along with biomass concentration of 1.53 g L^{-1} and lipid content of 31.33% (Sharma et al., 2021).

In harmony with existing literature, the present chapter investigates pilot scale reactor study for CME treatment via semi-continuous microalgae cultivation. Targeting multi-domain application strategy, the present chapter covers (i) reactor scale study through semi-continuous cultivation of candidate microalgae to investigate nutrient removal and lipid production, (ii) biodesalination and heavy metal remediation from NSCME using candidate microalgae and (iii) large scale implementation strategy of developed water treatment process at coal mine site using microalgae platform. The outcomes of present work will be able to develop long-term microalgae assisted low cost, efficient and sustainable CME treatment along with commercial scale biofuel production which can be integrated with coal mine closure plans in the near future.

4.2. Materials and methods

4.2.1 Indoor batch and semi-continuous cultivation

After a screening of candidate microalgae to treat CME, pilot scale study was performed by analysing algal biomass production and remediation of CME in two reactors, first, 10 L BCR having dimensions – 58 cm height, 16 cm outer diameter and 0.5 cm thickness and

second, 50 L ORP having dimensions – 80 cm length, 35 cm width and 26 cm height. Both systems were filled with 70% working volume of NSCME. Microalgae cultivation was examined in two successive stages as described: (i) batch mode till attainment of stationary phase, (ii) semicontinuous mode at three different HRTs of 4 d, 6 d and 9 d.

For semicontinuous cultivation, HRT was calculated according to Chu et al. (2015) as given (Eq. 4.1).

$$\mathrm{HRT} = \frac{2}{\mu} \tag{4.1}$$

Where μ is the specific growth rate (d^{-1}).

For initial inoculation in batch mode, NSCME acclimatized *C. pyrenoidosa* ($OD_{680\ nm}$ ≈ 2.0, inoculum size 10% v/v) was utilized as inoculum. The operating conditions such as temperature, light intensity and light-dark cycle were identical to flask study (section 2.3). In both reactors, 50 % (v/v) of culture medium in 2 d, 33.33% (v/v) of culture medium in 2 d and 33.33% (v/v) of culture medium in 3 d were replaced to achieve HRTs of 4 d, 6 d and 9 d, respectively. The semicontinuous mode was performed 22 d for HRT 4 d / HRT 6 d experiments and 27 d for HRT 9 d. To investigate the stability of the semicontinuous operations, five cycles of replacement were carried out in each HRT study. In each cycle, samples were collected on an alternate day basis from both reactors to assess growth in the form of biomass and lipid yields as well as nutrient removal in form of salinity and COD removal from CME.

4.2.2 Analytical methods

In a sequence of growth kinetic parameters calculation described in a previous chapter (section 3.2.4.1.1), biomass productivity (*BP*, g $L^{-1}d^{-1}$) during the microalgae growth time course was calculated according to Eq. 4.2.

$$BP = \frac{X_t - X_0}{t_t - t_0} \tag{4.2}$$

Where, X_t and X_0 are the final and initial biomass concentration (g L^{-1}) at the end of the growth phase (t_t) and at the start of growth phase (t_0), respectively.

The lipid productivity (LP, mg $L^{-1}d^{-1}$ was determined by using Eq. 4.3 as reported (Dickinson et al., 2013).

$$Lipid\ productivity\ (LP) = \frac{BP \times LC}{100} \quad (4.3)$$

Where, BP and LC are biomass productivity (g $L^{-1}d^{-1}$) and lipid content (w/w), respectively.

4.2.3 Lipid extraction and determination of fatty acid methyl esters composition

Lipid extraction from dried algal powder was performed using Bligh and Dyer's method via chloroform: methanol (2:1, v/v) extraction and quantification of lipid content was performed gravimetrically (Bligh and Dyer, 1959). The extracted lipid was dissolved in 0.6 M HCl in methanol to catalyze the reaction, as reported previously (Wicker et al., 2024). After transferring the prepared mixture into tubes, which were placed in a water bath set at temperature 85 °C. Proceeding one h reaction, tubes were cooled at room temperature. As a solvent, n-hexane was used to extract FAMEs and further analysis was performed using gas chromatography (GC 7890A, Agilent, Santa Clara, California, US) and mass spectroscopy (MS 5975C, Agilent, Santa Clara, California, US), equipped with silica capillary column (HP-5 MS, Agilent) with dimensions 30 m×0.25mm×0.25µm. The initial oven temperature was set to 60 °C for 5 min and then increased to 150 °C and 220 °C with 2–2 min hold time till final temperature of 275 °C at a heating rate of 20 °C/min. Helium was utilized as a carrier gas in split mode with a split ratio of 10:1 at 1.5 mL/min flow rate. A 2 µL sample was injected at an injection port temperature of 280 °C and the MS transfer line temperature was maintained at 280 °C. Mass spectra range from 40 to 700 with an acquisition rate of 20 spectra per second was maintained using electron ionization of 70 eV.

4.2.4 Statistical analysis

One way analysis of variance and Tukey's Honestly significant difference (HSD) test was applied for statistical investigation of % COD removal and % salinity removal at different HRTs. The test was performed by applying RStudio software (version 4.3.0). The statistical difference between the means of different groups was assessed by setting a significance level of $\alpha = 5\%$ with $p < 0.05$.

4.3 Results and discussion

Considering the promising results of the flask scale study for biomass production and CME treatment as described in section 3.3.2, the potential biomass production and CME treatment was further investigated in BCR and ORP via semi-continuous cultivation at different HRTs (Fig. 4.1). In strong agreement of previous reported studies, bubble column and raceway system are considered economically viable options for pilot scale algal biomass production and wastewater treatment (Nordio et al., 2023).

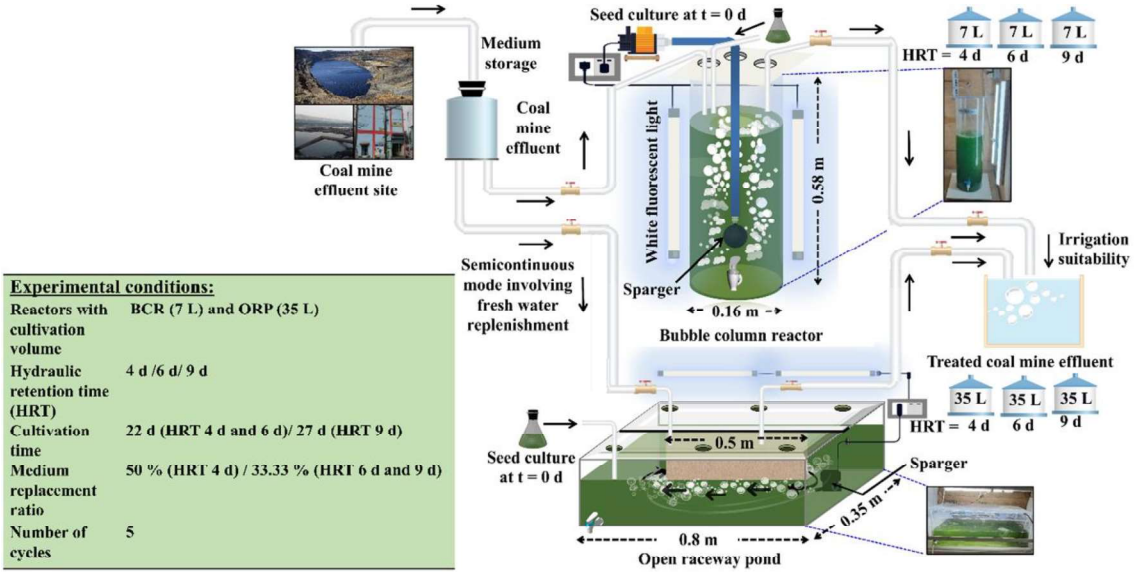

Fig. 4.1 Schematic representation of the indoor experimental set-up of bubble column reactor and open raceway pond for semi-continuous treatment of coal mine effluent.

4.3.1 Biomass and lipid productivities of *C. pyrenoidosa* sp. in semi-continuous cultivation

Semi-continuous cultivation facilitates higher cell density, higher lipid productivity and better process monitoring over batch mode, ultimately leading to reduced operating cost for biomass production at pilot scale (Yu et al., 2021). Based on kinetic growth parameters obtained in batch cultivation, semi-continuous operation was performed at specific HRTs. The Fig. 4.2 illustrates the dynamics of microalgae biomass (g L^{-1}) and lipid content (%) at three HRTs of 4 d, 6 d and 9 d. The growth of *C. pyrenoidosa* sp. in NSCME was consistent for the entire batch cultivation mode with the optimum biomass concentration of 2.5 g L^{-1} and μ of 0.33 d^{-1} (Fig. 4.2). In semi-continuous cultivation, HRT 4 d was maintained by 50% (v/v) culture medium replacement at every 2 d interval which lead to gradual decrease in biomass concentration after every semi-continuous cycle (throughout 5 cycles) as shown in Fig. 4.2a and b. The short HRT (4 d) showed a negative trend for biomass and lipid productivity, indicating that microalgae could not acclimatize within two cultivation days and did not achieve the optimum biomass concentration as attained in batch cultivation due to frequent medium replacement (Tan et al., 2018). The maximum biomass concentration of 5.7 g L^{-1} in BCR and 4.5 g L^{-1} in ORP was observed at HRT 6 d (Fig. 4.2c and d). The 33.33% (v/v) medium replacement at every 2 d interval is sufficient to readjust semi-continuous turbulence and attain optimum biomass concentration with continuous maintenance of log phase growth (Tan et al., 2018). The positive trend with continuous increment in biomass concentration was observed at HRT 6 d (Fig. 4.2c and d) with maximum average biomass productivity of 950 mg L^{-1} d^{-1} in BCR and 728.4 mg L^{-1} d^{-1} in ORP (Fig. 4.3). The similar positive trend in biomass profile was observed for HRT 9 d with 33.33% (v/v) medium replacement at every 3 d interval which shows maximum biomass concentration of 4.9 g L^{-1} in BCR and 3.9 g L^{-1} in ORP which lie in between HRT 6 d and HRT 4 d (Fig. 4.2e and f). Similarly, the average biomass

productivity for HRT 9 d (574.7 mg L^{-1} d^{-1} in BCR and 447.2 mg L^{-1} d^{-1} in ORP) lay between HRT 6 d and HRT 4 d (Fig. 4.3).

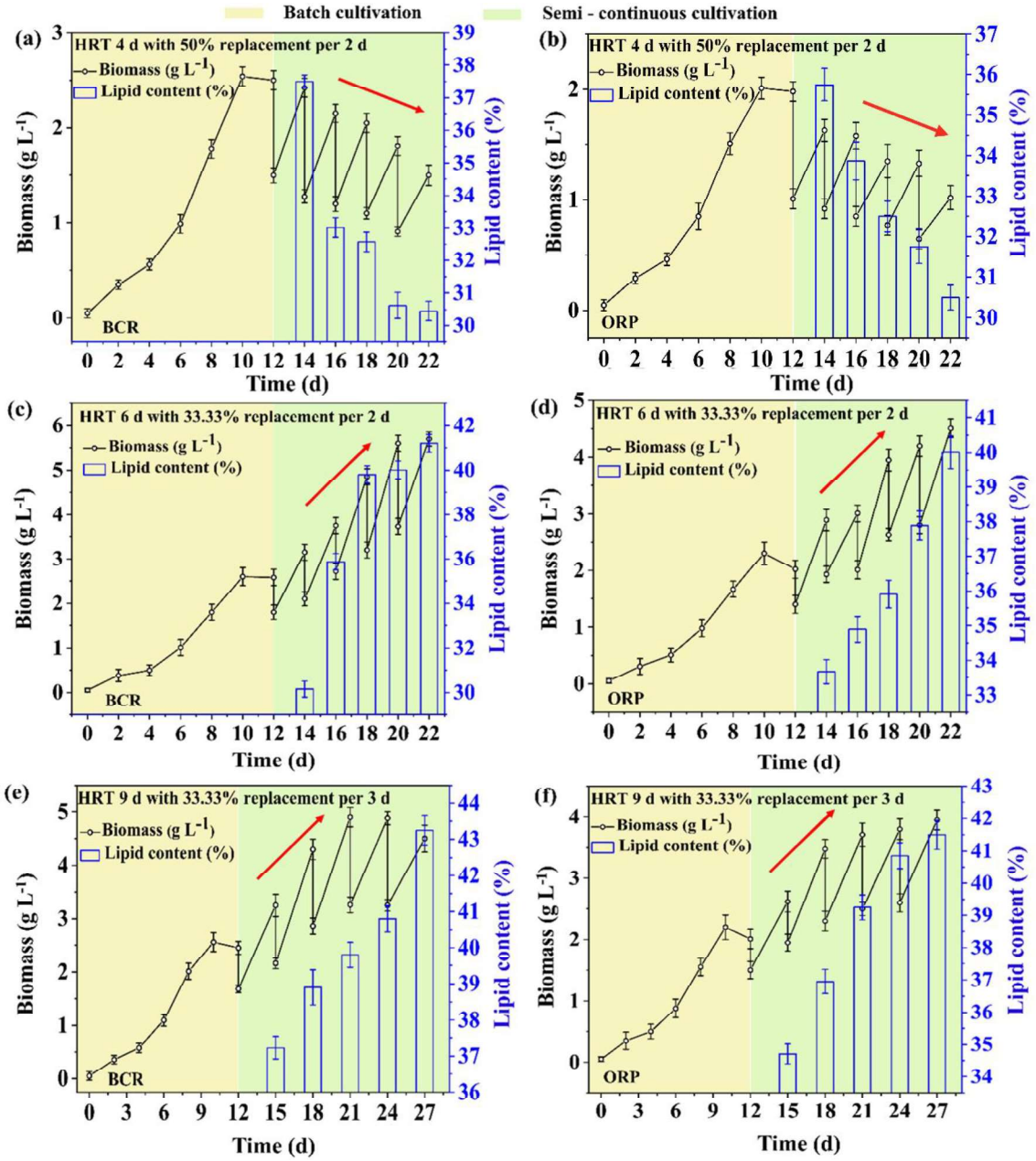

Fig. 4.2 Biomass concentration (g L^{-1}) and lipid contents (%) of candidate microalgae *Chlorella pyrenoidosa* in nutrient supplemented coal mine effluent cultivated in semi-continuous mode (a,c,e) Bubble column reactor (BCR), (b,d.f) Open raceway pond (ORP).

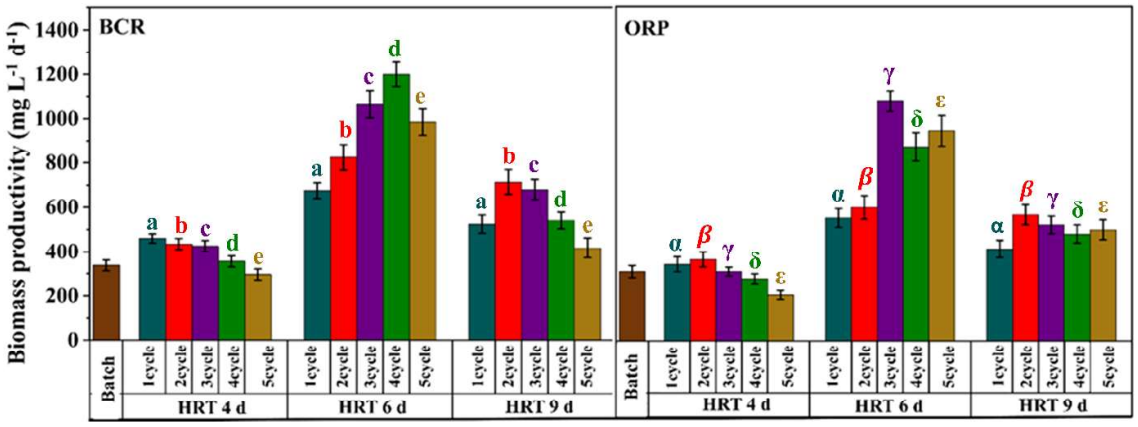

Fig. 4.3 Biomass productivity (mg L−1 d −1) of microalgae at different hydraulic retention time (HRT) during batch and semi-continuous cultivation mode in bubble column photobioreactor (BCR) and open raceway pond (ORP). Tukey's test (α = 5%) was performed with $p < 0.05$ among different groups. Different letters indicate statistically significant differences.

Investigating lipid content (%) at different HRTs, it was observed that HRT 4 d showed relatively low lipid content and negative trend in accumulated lipid from cycle 1 to cycle 5 due to the absence of nitrogen starvation condition as more frequent feeding (2 d) facilitate sufficient nitrogen to favor microalgal cell growth (Fig. 4.3a and b). Amongst different HRTs, HRT 9 d provided a maximum lipid content of 1.9 g L^{-1} (43.25%, w/w) in BCR and 1.6 g L^{-1} (41.5%, w/w) in ORP as nitrogen depletion conditions were maintained at longer HRT in both reactors. Similar to HRT 9 d, HRT 6 d also showed a positive trend in lipid profile from cycle 1 to cycle 5, which lie in between HRT 9 d and HRT 4 d (Fig. 4.2). In both the systems (BCR and ORP), moderate HRT 6 d showed best performance with maximum biomass productivities of 950 mg L^{-1} d^{-1} in BCR and 728.4 mg L^{-1} d^{-1} in ORP. The results are in strong agreement of another semi-continuous study of *C. pyrenoidosa* sp. cultivated in anaerobic digested starch processing wastewater, which reported moderate HRT 4 d in between 2 d and 10 d, showing high biomass productivity of 342.6 ± 12.8 mg L^{-1} d^{-1} and lipid productivity of 43.37 ± 12.8 mg L^{-1} d^{-1} (Chu et al., 2015). A semi-continuous study of *S. obliquus* cultivation in dairy wastewater reported a significant impact of HRT based culture upon biomass/lipid

productivity, which showed 220 mg L^{-1} d^{-1} average biomass productivity with 31.45–35.74% lipid accumulation at 6 d HRT (Ling et al., 2019).

4.3.2 Nutrient removal performance at different hydraulic retention time in semi-continuous cultivation

In the present study, coal mine water treatment, specifically desalination, was performed by cultivating candidate *C. pyrenoidosa* in NSCME via semi-continuous mode. The nutrient removal performance, i.e., salinity removal in terms of EC (mS cm^{-1}) and COD removal of NSCME was performed in semi-continuous mode started as a batch culture with the initial EC of 5.2 mS cm^{-1} and COD of 285 mg L^{-1} for 12 days. Further, batch mode was switched to semi-continuous mode with three different operating strategies of HRT 4 d, 6 d and 9 d in both reactors (BCR and ORP). The dynamics of EC removal (mS cm^{-1}) and COD removal (mg L^{-1}) at different HRTs were investigated throughout five cycles (Fig. 4.4a – f). The average final concentration of the nutrients (EC and COD) was higher under 50% (v/v) medium at every 2 d (HRT 4 d) than those of 33.33% (v/v) medium replacement at every 2 d (HRT 6 d) and every 3 d (HRT 9 d) as shown in Fig. 4.4a and b. The longest HRT (9 d) had the maximum COD removal efficiency (96.5% in BCR and 94.2% in ORP) as well as maximum salinity removal efficiency (93% in BCR and 92% in ORP) (Fig. 4.4e and f).

The moderate HRT (6 d) also showed suitable COD removal efficiency (95.8% in BCR and 92.9% in ORP) as well as salinity removal efficiency (90.9% in BCR and 90% in ORP) (Figs. 4.4c and d). Performing Tukey test (α =5% $p < 0.05$), it was observed that there is no significant difference between HRT 9 d and HRT 6 d group data as shown in Table 4.1. However, HRT 4 d showed relatively lower nutrient removal efficiencies (% COD removal and % salinity removal) with significant differences from HRT 9 d and HRT 6 d data (Table 4.1).

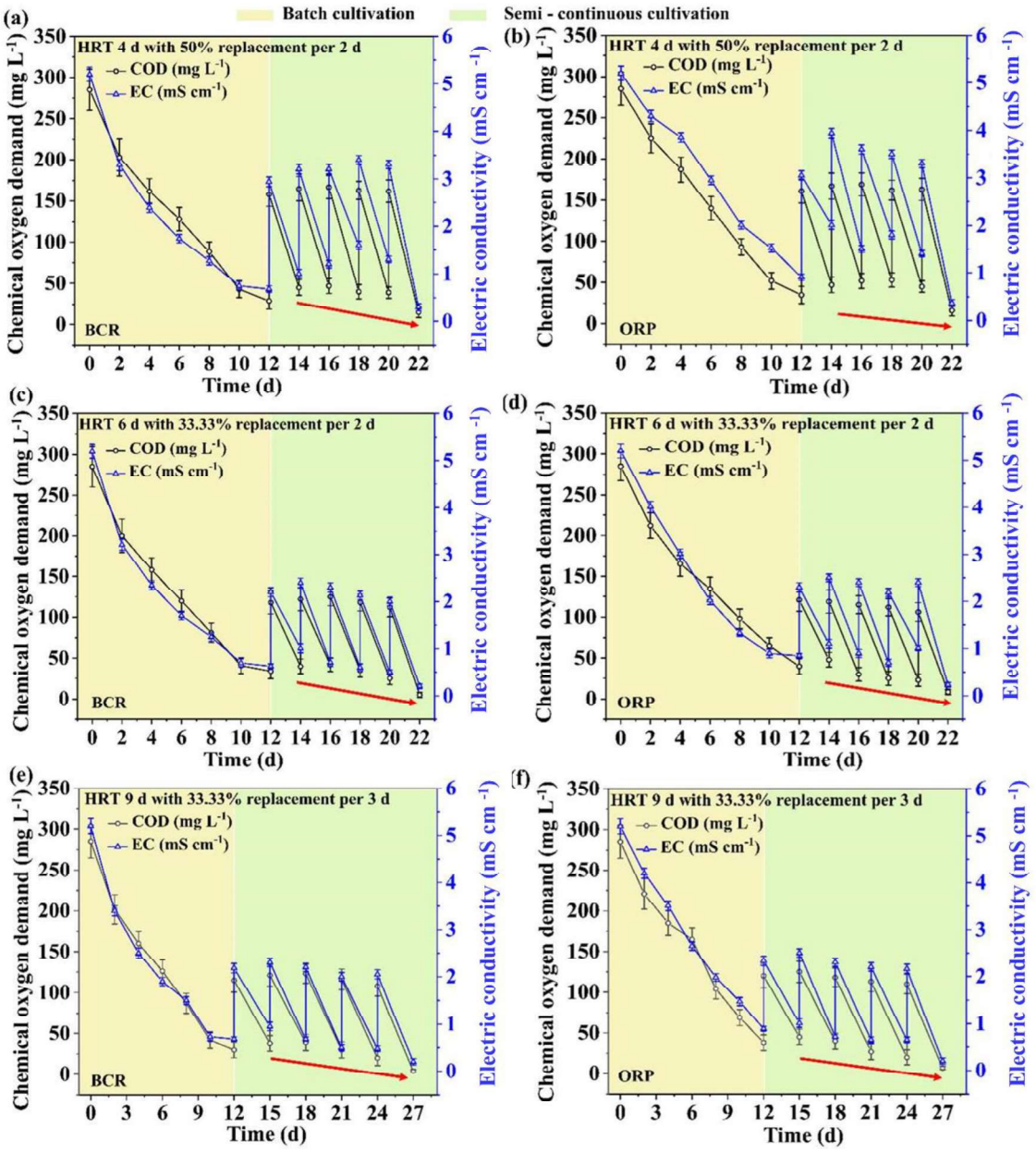

Fig. 4.4 Chemical oxygen demand (mg L^{-1}) and electric conductivity (mS cm^{-1}) variation of nutrient supplemented coal mine effluent during semi-continuous mode (a,c,e) Bubble column photobioreactor (BCR) (b,d,f) Open raceway pond (ORP). All observed values of responses were mean values of triplicates ± standard deviation.

Contrary to nutrient removal efficiency results, HRT 4 d showed maximum COD removal rates in both reactors (62.9 mg L^{-1} d^{-1} in BCR and 60.7 mg L^{-1} d^{-1} in ORP) as well as maximum salinity removal rates in both reactors (1.32 mS cm^{-1} d^{-1} in BCR and 1.06 mS cm^{-1} d^{-1} in ORP) as depicted in Table 4.1.

The probable reason is that short HRT handles a higher capacity of water at short time resulting higher nutrient removal rates (Chen et al., 2021). A similar trend of nutrient removal efficiency and nutrient removal rate was observed in semi-continuous cultivation of *C. sorokiniana* AK-1 in piggery wastewater, showing a maximum COD removal efficiency of 93% in 6 d and a maximum COD removal rate of 762 mg $L^{-1}d^{-1}$ in 4 d (Chen et al., 2021).

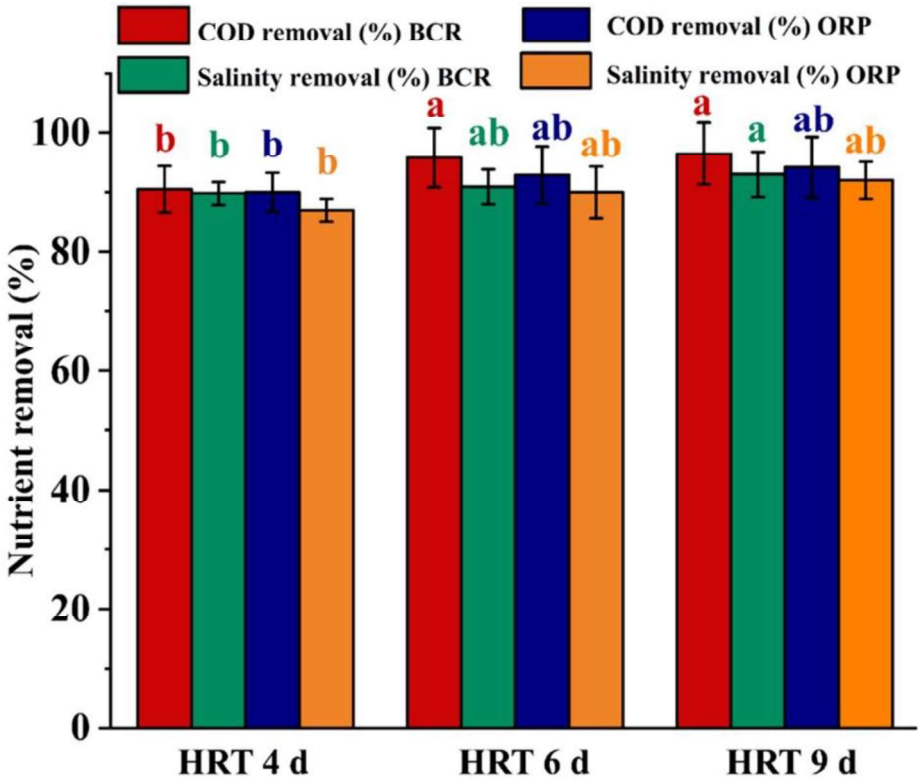

Fig. 4.5 Nutrient removal (%) at different hydraulic retention time (HRT) during semi-continuous cultivation mode in bubble column photobioreactor (BCR) and open raceway pond (ORP). Tukey's test ($\alpha = 5\%$) was performed with $p < 0.05$ among different groups. Different letters indicate statistically significant differences.

Both the reactors (BCR and ORP) exhibited best operating strategy as HRT 6 d performing maximum biomass productivity with relatively higher lipid accumulation and stable and effective nutrient removal. In the present study, a suitable HRT based semi-continuous operation ensures long-term sustainable performance for coal mine water treatment for scale-up and commercialization in future studies.

Table 4.1 Average nutrient removal performance of all cycles (1–5) under semi-batch operation with different medium replacement ratios.

NSCME loading in each cycle	HRT (d)	Average nutrient removal of all 5 cycles of different hydraulic retention time							
		COD removal rate ($mg\ L^{-1}\ d^{-1}$)		COD removal efficiency (%)		Salinity removal rate ($mS\ cm^{-1}\ d^{-1}$)		Salinity removal efficiency (%)	
		BCR	ORP	BCR	ORP	BCR	ORP	BCR	ORP
50% in 2 d	4	62.9 ± 2.5	60.7 ± 1.8	90.5 ± 3.1	90.0 ± 2.8	1.32 ± 0.03	1.06 ± 0.05	89.8 ± 3.01	87.0 ± 2.87
33.33% in 2 d	6	44.8 ± 1.7	44.15 ± 1.5	95.8 ± 3.2	92.9 ± 4.1	0.81 ± 0.03	0.78 ± 0.03	91.0 ± 4.5	90.0 ± 3.1
33.33% in 3 d	9	30.1 ± 1.05	29.7 ± 0.9	96.5 ± 3.8	94.16 ± 5.2	0.6 ± 0.02	0.55 ± 0.02	93.0 ± 4.8	92.0 ± 4.01

All observed values of responses were mean values of triplicates ± standard deviation; NSCME: Nutrient supplemented coal mine effluent; HRT: Hydraulic retention time; COD: Chemical oxygen demand; BCR: Bubble column reactor; ORP: Open raceway pond.

4.3.3 Fatty acid methyl ester analysis of candidate *C. pyrenoidosa* sp. cultivated in NSCME

The lipid transesterification to fatty acid methyl ester was further analyzed through Gas chromatography-mass spectrometry. The fatty acid composition of candidate *C. pyrenoidosa* sp. cultivated in NSCME is shown in Table 4.2. These fatty acids are mainly distributed as saturated fatty acids (SFA), monounsaturated fatty acid (MUFA) and polyunsaturated fatty acids (PUFA), comprising 99.83% of total lipids.

The FAME analysis revealed the presence of main MUFA and PUFA such as C16:1 (7.8), C17:1 (10.1), C18:1 (10.6), C18:2 (10.6), C18:3 (10.5), C20:2 (4.83). The bio-oil contains SFA such as C16:0 (6.5), C17:0 (5.1), C18:0 (9.4), C22:0 (5.5) and C24:0 (9.5). The fatty acids composition and proportion of MUFA and PUFA fatty acids can crucially impact biodiesel characteristics such as cetane number (CN), cold flow plug properties and oxidative stability. The long-chain saturation factor at high level significantly affects the cold flow behavior of biodiesel (Xiao et al., 2019). The degree of unsaturation is correlated to number of

double bonds in the fatty acid chain that enhance oxygen interaction when exposed to air and strongly affect the oxidative stability of biodiesel (Xiao et al., 2019).

Table 4.2 Summary of the fatty acid methyl ester profile of *C. pyrenoidosa* sp. harvested after end cycle of HRT 6 d through semi-continuous cultivation in NSCME.

Fatty acid methyl esters	**Nature**		**Percentage of composition (%)** [a]
Pentadecanoic acid, methyl ester	C15:0	SFA	2.01 ± 0.2
Cis-10 pentadecanoic acid, methyl ester	C15:1	MUFA	3.5 ± 0.3
Hexadecanoic acid, methyl ester	C16:0	SFA	6.5 ± 0.5
9-Hexadecenoic acid, methyl ester	C16:1	MUFA	7.8 ± 0.61
Heptadecanoic acid, methyl ester	C17:0	SFA	5.1 ± 0.41
Cis-9-Heptadecenoic acid, methyl ester	C17: 1	MUFA	10.1 ± 1.2
Stearic acid, methyl ester	C18:0	SFA	9.4 ± 1.01
Octadecenoic acid, methyl ester	C18:1	MUFA	10.6 ± 2.1
6,9-Octadecadienoic acid, methyl ester	C18:2	PUFA	10.6 ± 2.3
9,12,15-Octadecatrienoic acid, methyl ester	C18:3	PUFA	10.5 ± 1.5
Cis-11,14-eicosadienoic acid, methyl ester	C20:2	PUFA	4.83 ± 0.7
5,8,11,14-Eicosatetraenoic acid, methyl ester	C20:4	PUFA	0.98 ± 0.12
Docosenoic acid, methyl ester	C22:0	SFA	5.5 ± 0.25
Cis-4,7,10,13,16,19- Docosahexaenoic acid, methyl ester	C22:6	PUFA	0.76 ± 0.05
Tetracosanoic acid, methyl ester	C24:0	SFA	9.5 ± 0.87
Cis-15-tetracosenoic acid, methyl ester	C24:1	MUFA	1.8 ± 0.15
Octacosanedioic acid, methyl ester	C28:0	SFA	0.35 ± 0.08
Biodiesel properties [b]			
UFA/SFA	1.6		
SV	193.33		
IV	91.52		
CN	53.94		

[a]All observed values of responses were mean values of triplicates ± standard deviation; [b] mean values of triplicates (standard deviation < 3%); SFA: Saturated fatty acid; UFA: Unsaturated fatty acid; MUFA: Monounsaturated fatty acid; PUFA: Polyunsaturated fatty acid; Biodiesel fuel parameters included SV: saponification value; IV: iodine value; CN: cetane number.

To investigate the viability of microalgal lipids as feedstock of biodiesel, the key characteristics, cetane number (CN), saponification value (SV) and iodine value (IV), were analyzed following European biodiesel standard (EN-14214). High CN of biodiesel is correlated with combustion quality and provides shorter ignition delay time in internal combustion engines with enhanced ignition and decreased NO_x emissions (Knothe and Razon, 2017). Whereas, IV should be less than 120 which is considered as degree of unsaturation of

the bio-oil (EN-14214 standard). A high IV is considered as non desirable property and related to low oxidative stability of the fuel (Knothe and Razon, 2017).

In present study, the lipid profile of *C. pyrenoidosa* cultivated in NSCME showed the CN (53.94) and IV (91.52) as per international fuel quality standards (ASTM D6751 and EN 14214), which indicated acceptable biodiesel quality of microalgal lipid utilising CME (Table 4.2).

These results are quite comparable to FAME analysis of microalgae species cultivated in different waste waters such as *Scenedesmus* sp. in dairy effluent showing CN – 56.59 and IV – 67.64 (Pandey et al., 2019) as well as *Haematococcus* sp. in seafood processing effluent with CN – 49.04 and IV – 105.77 (Jehalee et al., 2024).

4.3.4 FTIR analysis of microalgal biomass, lipid extracted microalgal biomass and oil

In semi-continuous microalgae cultivation, different samples such as *C. pyrenoidosa* cultivated in different medium (BG-11 and NSCME), lipid extracted microalgal biomass, extracted lipid and FAME were analyzed via FT-IR spectroscopy to depict functional groups present in it. The FTIR spectra of microalgae cultivated in BG-11 showed prominent peaks at 1700–1500 cm^{-1} due to N–H, C=N and C=O bending assigned for amide-I, amide-II and carbonyl bonding from proteins respectively (Fig. 4.6a). These characteristic peaks are identical in *C. pyrenoidosa* cultivated in both BG-11 and NSCME medium (Fig. 4.6a and b). The spectra from 3100 to 2800 cm^{-1} corresponds to presence of lipid in microalgae cultivated in both BG-11 and NSCME as reported in other studies (Kothari et al., 2013). The relatively sharp peaks at 2927– 2850 cm^{-1} indicated lipid content increment in NSCME grown microalgae due to maintaining nutrient stress conditions (Fig. 4.6b). Further, the identical peak (2927–2850 cm^{-1}) is reduced in lipid extracted microalgal biomass, which shows that lipid was successfully extracted (Fig. 4.6c). These results strongly agree with previously reported FTIR analysis of lipid extracted *Scenedesmus* sp. cultivated in dairy effluent (Pandey et al., 2019).

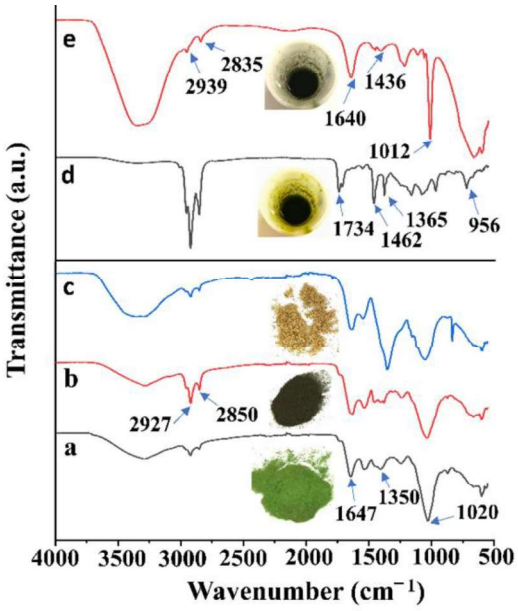

Fig. 4.6 FTIR spectrum of (a) BG-11 grown microalgae (b) Nutrient supplemented coal mine effluent grown microalgae (c) De-oiled nutrient supplemented coal mine effluent grown microalgae (d) Extracted lipid from nutrient supplemented coal mine effluent grown microalgae (e) Fatty acid methyl ester from nutrient supplemented coal mine effluent grown microalgae.

The infrared spectra of microalgal lipid cultivated in NSCME is very much identical to biodiesel indicating strong ester peak at 1462 cm^{-1}(C=O vibration) as reported in previous studies (Fig. 4.6d). The multiple peaks in 956–1365 cm^{-1} corresponding to C–O vibration is also mentioned in soybean oil (Kothari et al., 2013). Further, peaks in the range of 1743–1734 cm^{-1} correspond to > C=O stretching which is identical to soybean oil as shown in Fig. 4.6d (Forfang et al., 2017).

The FTIR spectra of bio-oil obtained from microalgal sources showed a shifted band position of methoxycarbonyl group when compared to the carbonyl band in the soybean oil and diesel (Fig. 4.6d). Further, FAME spectra show peak around 2939 cm^{-1} and 2835 cm^{-1} respectively assigned for C–H stretch for alkanes (Fig. 4.6e) in strong agreement of reported studies (Ogbu and Ajiwe, 2016). Multiple transmittance peaks obtained at 1200–1000 cm^{-1} as shown in Fig. 4.6e may correspond to stretching vibration of (CC(=O)–O) bonds of ester and asymmetric stretching vibration of (O–C–C) bonds as reported by previous studies also (Patil

et al., 2011). Further, the peaks around 1436 cm^{-1} may be due to methyl C–H asymmetric bending (Fig. 4.6e).

Therefore, the FTIR analysis of lipid extracted from *C. pyrenoidosa* sp. cultivated in NSCME strengthens the presence of fatty acids, indicating its potential as biodiesel feedstock.

4.3.5 Biodesalination and heavy metal remediation from NSCME using *C. pyrenoidosa*

In present study, the desired function of microalgae-based wastewater treatment is to remove excess metal/heavy metal load (Fe, Cu, Pb and Cr) and salt stress (Na) from saline coal mine water. The microalgae-based desalination is an emerging trend and a promising alternative of conventional methods due to excellent salt and metal removal efficiency (Leong and Chang, 2020). Considering EPA and FAO permissible limits for irrigation (50 for COD and 2 mS/cm for EC), biodesalination of NSCME was successfully achieved as evidenced by significant reduction in EC and COD (Fig. 4.5). After excellent nutrient removal performance by *C. pyrenoidosa* in NSCME via semi-continuous mode, the final concentration of heavy metals and salt was investigated in treated water through ICP-MS analysis as well as field emission scanning electron microscopy (FE-SEM) / EDS analysis.

Biosorption of salt particles and metals/heavy metals on the surface of *C. pyrenoidosa* was confirmed by comparing the FE-SEM and EDS results of microalgae harvested after end cycle of HRT 6 d through semicontinuous cultivation and microalgae inoculated at start of cycle (t=0 d) as shown in Fig. 4.7. The FE-SEM results confirmed the surface topographical variation before and after desalination showed evidence of sediment deposition during *C. pyrenoidosa* cultivation in NSCME as shown in Fig. 4.7a. The EDS analysis confirmed that excluding conventional elements (C and O), a low amount (% weight fraction) of Na^{+} (0.4%) and Mg^{2+} (1.2%) were present in the microalgae inoculated at the start of experiment (t = 0 d) as shown in Fig. 4.7b.

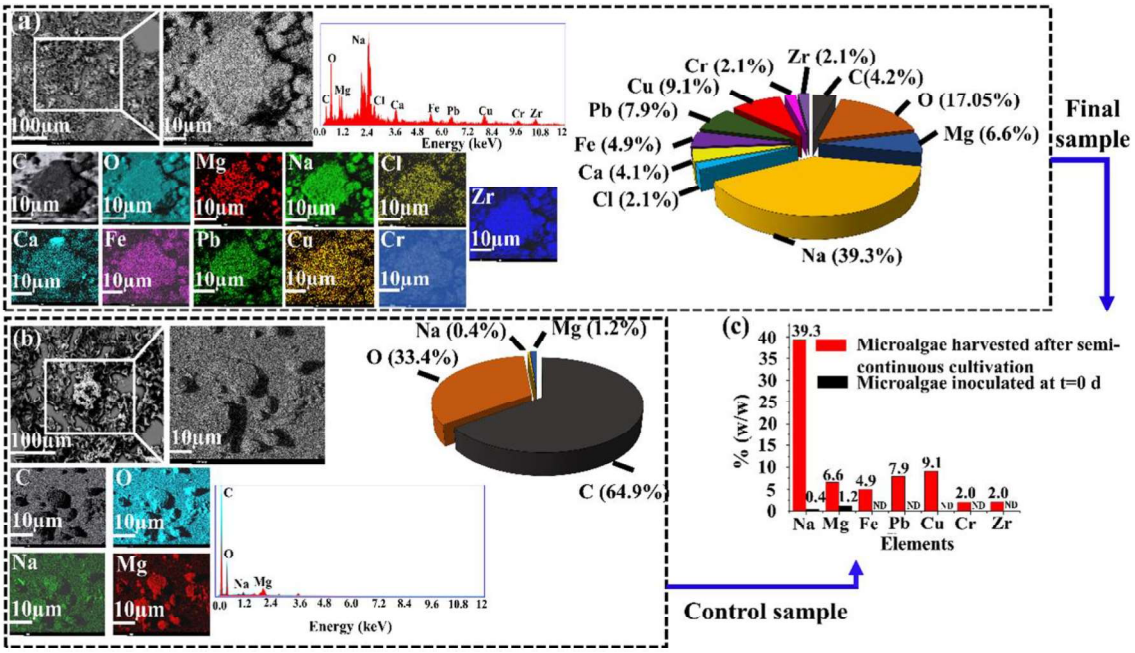

Fig. 4.7 SEM micrograph and elemental mapping of salts and heavy metals assimilated in microalgae *C. pyrenoidosa* (a) harvested after end cycle of HRT 6 d through semi-continuous cultivation (b) microalgae at start of cycle (t = 0 d) (c) comparison of elemental mapping at end cycle of HRT 6 d and t = 0 d. *ND – not detected.*

Further, this microalgae sample has not accumulated metal/heavy metal such as Fe^{2+}, Cu^{2+}, Pb^{2+} and Cr^{2+}. Although, microalgae sample at end of experiment showed salts in highly excess amount (% weight fraction) as Na^{+} (39.3%) and Mg^{2+} (6.6%) which confirmed the adsorption of these salts on the surface of *C. pyrenoidosa* as successful biodesalination of NSCME (Fig. 4.7a). Further, excess accumulation of metal ions (% weight fraction) as Fe^{2+} (4.9%), Pb^{2+} (7.9%), Cu^{2+} (9.1%) and Cr^{2+} (2.0%) were absorbed in microalgae sample after desalination (Fig. 4.7c). The EDS data quantifying biomass ion content highlighted substantial increment in salt and metal ions on the cell surface during experiment which is in agreement with EDS results of recently reported biodesalination of saline aquaculture wastewater using microalgae *Arthrospira platensis* and *D. salina* (Mirzaei et al., 2024). In another study, *Spirulina* sp. showed the ability to remove salt/ metal ions such as Na^{+}, K^{+} and Co^{2+}, Cu^{2+}, Mn^{2+} and Zn^{2+} (Dmytryk et al., 2014). These metal ions binding on the microalgal surface of

C. pyrenoidosa might be understood with the aspect of excessive binding sites provided by large surface area of algal cells as confirmed by other studies (Sharma et al., 2020). The salt ions and heavy metal ions binding on algal cells could be attributed by biodesalination processes such as bioadsorption (physical adherence) and bioaccumulation (energy derive uptake) of ions on the microalgae surface (Patel et al., 2021). After successful biodesalination/ metal ions removal by using *C. pyrenoidosa*, the final salt and metal concentration in treated NSCME is reconfirmed by ICP-MS analysis to ensure the irrigation suitability of treated water (Table 4.3). These findings suggest that the microalgae assisted coal mine water desalination can also be investigated in a larger system (outdoor cultivation).

Table 4.3 Comparative assessment of ICP-MS results of NSCME desalination.

Elements (mg L^{-1})	NSCME $_{Before\ desalination}$	NSCME $_{After\ desalination}$	% removal
Na	250 ± 2.5	17.5 ± 0.5	93.0
Mg	38 ± 0.9	6.9 ± 0.45	81.8
Fe	8.78 ± 0.5	0.88 ± 0.001	89.9
Pb	0.65 ± 0.05	0.10 ± 0.002	84.6
Cu	2.05± 0.07	0.21 ± 0.009	89.8
Cr	0.18 ± 0.007	0.03 ± 0.001	83.3

NSCME: Nutrient supplemented coal mine effluent.

4.3.6 Large scale implementation strategy of developed water treatment process at coal mine site

Considering efficient coal mine water treatment by *C. pyrenoidosa* at reactor scale, the large-scale microalgae cultivation can be planned at coal mine sites that offer sufficient suitable land and water resources at higher solar radiation geographies (Levett et al., 2023). Large-scale microalgal biomass production will facilitate efficient CO_2 capturing and saline mine water treatment for irrigation suitability with massive biomass and lipid production (Levett et al., 2023). The present study plans in situ treatment of coal mine water through direct microalgae injection into the local water bodies/ shallow coal mine water reservoirs (approximately 30–40 cm depth) instead of pumping out water for conventional water treatment through treatment

plant as shown in Fig. 4.8. The large-scale microalgae cultivation at coal mine site assumed 50 ha microalgae production facility at coal mine site. The best results of indoor semi-continuous cultivation showing maximum average biomass productivity of 950 mg $L^{-1}d^{-1}$ (BCR, HRT 6 d) is applied to calculate microalgal aerial productivity of 0.02 kg m^{-2} d^{-1} for design consideration of 7 L working volume BCR (58 cm height, 16 cm outer diameter and 0.5 cm thickness as described in sec. 2.4).

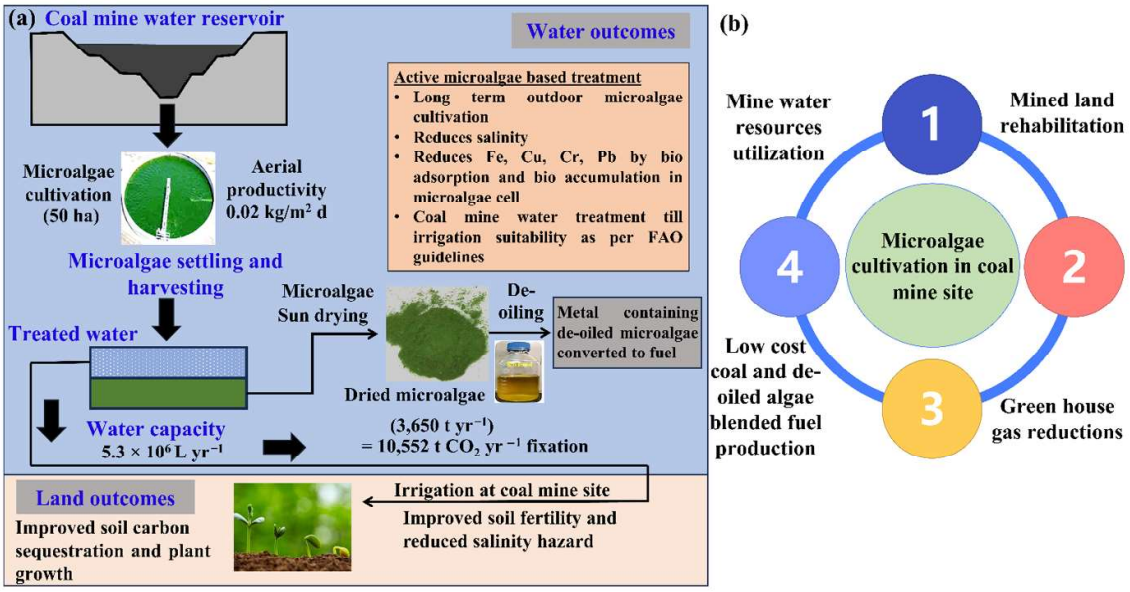

Fig. 4.8 Long term outdoor microalgae cultivation in coal mine site (a) flow diagram representing active microalgae-based wastewater treatment with possible water and land outcomes (b) potential environmental and social implications of microalgae production at coal mine site.

The obtained microalgal aerial productivity (0.02 kg m^{-2} d^{-1}) is scaled up to a 50 ha microalgae production facility at the coal mine site. These calculations interpret 1×10^{4} kg d^{-1}/ 3650 t yr^{-1} microalgae production at coal mine site (Fig. 4.8a). A potential concern to cultivate microalgae in coal mine sites evolves enhanced biomass production and direct water treatment for irrigation suitability in nearby coal mine area. The maximum CO_2 fixation rate of candidate microalgae *C. pyrenoidosa* will result nearly 10,552 t yr^{-1} CO_2 fixation at coal mine site, which reflects as an attractive low-cost CO_2 capturing strategy leads to a substantial amount of

greenhouse gas reduction through a well-constructed microalgae production facility holding 30–35 yr lifespan. Considering semi-continuous cultivation (HRT 6 d for 5 cycles) as an applied strategy, the treated water capacity will be approximately 5.3×10^6 L yr^{-1}. The large volume of treated coal mine water must be investigated with commercial water reusability guidance and further used for irrigation at nearby coal mine sites. The long-term irrigation practice (> 10 yr) will provide (i) improved soil fertility (ii) reduced salt stress for crop growth (iii) increased soil carbon sequestration (iv) revegetation and reforestation at coal mine site (Fig. 4.8 a). After achieving coal mine water treatment as desired objective, the sun dried microalgal biomass (approximately 3650 t yr^{-1}) may be utilized for bio-diesel production through lipid extraction (following Bligh and Dyer approach). Further, de-oiled microalgae constituting 37–40% of total microalgae biomass may be completely utilized via mechanical conversion such as briquetting process to produce solid fuels (Rawat and Kumar, 2023a) as well as thermochemical conversion such as pyrolysis/ co-pyrolysis to produce bio-oil (Rawat et al., 2024b).

Although, coal mine effluent site is the natural habitation of a very limited bacterial community due to high salinity, heavy metal contamination and other stress conditions. In this direction, *Bacillus* sp. (*B. pseudomycoides*, *B. siamensis*) is among the few culturable bacterial community in coal mine site (Rawat et al., 2024c). In contrary to that microalgae are considered as potential salt-tolerant hyper-accumulators, able to grow in different type of coal mine effluent exhibiting wide range of salinity from 2−20 g L^{-1} (Rawat et al., 2024c). Integrating microalgal biomass/biofuel production with mine water treatment at mine site may be a potential solution for developing eco-friendly, sustainable and cost-effective processing. The long-term potential environmental benefits are (i) carbon capture, utilisation and storage in microalgae biomass, (ii) regulation of greenhouse gas emission, (iii) increased soil carbon sequestration, (iv) improved plant growth resulting revegetation and reforestation at coal mine

sites (Fig. 4.8b). One step ahead, scaled up microalgal biomass production and development of microalgae biorefinery would be expected to support local employment to miners even after closure of mine.

4.4 Conclusion

Present chapter concludes significant opportunities and potential benefits through integrating microalgae production and mine water treatment. The candidate microalgae *C. pyrenoidosa* (NCIM 2738) was investigated to explore lipid production potential and desalination efficiency using NSCME via semi-continuous cultivation mode at different HRTs of 4 d, 6 d and 9 d. In BCR, maximum biomass concentration of 5.7 g L^{-1} and subsequently maximum biomass productivity of 950 mg L^{-1} d^{-1} was maintained at HRT 6 d due to highest cell growth rate and stable biomass accumulation. Evaluating dynamics of nutrient removal, it was observed that HRT 9 d had maximum COD removal efficiency (96.5% in BCR) and maximum salinity removal efficiency (93% in BCR). Moreover, EDS results revealed excess accumulation or absorption of salt ions (Na^{+}/ Mg^{2+}) and metal ions (Fe^{2+}, Pb^{2+}, Cu^{2+} and Cr^{2+}) in microalgae sample indicating successful desalination from NSCME which was further reconfirmed by ICP-MS analysis. In the next stage, coal mine sites with suitable land, water resources and high solar radiation geographies will be considered excellent for long-term outdoor microalgae production facility to treat CME and provide environment benefits such as increased soil carbon sequestration and revegetation/reforestation at coal mine site. The present microalgae assisted mine water treatment strategy offers sustainable practices in coal industry by reducing water footprint of mining and providing effective, sustainable solutions in the long run. Microalgal platforms employ a circular economy approach at the mining site to achieve large-scale water treatment for irrigation and commercial biofuel production, fulfilling desired SDGs.